Combinatorial Rheology of Branched Polymer Melts

R. G. Larson

Department of Chemical Engineering, University of Michigan, Ann Arbor, Michigan 48109-2036

Received April 20, 2000; Revised Manuscript Received September 8, 2000

ABSTRACT: An algorithm is presented for predicting the linear viscoelasticity of polydisperse polymers containing long side branches with arbitrary distributions of branch length and branch location along a backbone. The algorithm gives semiquantitative predictions of literature data for a wide range of polybutadiene melts, including monodisperse linear, star, mixed linear and star, pom-pom, and comb polymers. Huge differences (several orders of magnitude) are predicted in zero-shear viscosities for samples that have the same weight-average molecular weight (200 000) and the same branching fraction but have different branching structures. It is shown that information on branching structure can be inferred by combinatorially measuring rheological properties on series of blends of the branched polymer with a linear, or well-defined branched, polymer.

I. Introduction

One of the most important practical problems in the field of polymer melt rheology is the characterization of long-chain branching, or "LCB," and predicting its effect on melt rheology. LCB characterization requires measurement of the density of branch points, branch lengths, and (if possible) the locations of the branches along the polymer "backbone" or along other branches. The characterization problem is closely linked with the problem of rheological prediction because rheology is the most sensitive indicator of the degree and type of LCB. Rheological measurements of shear or extensional melt viscosity manifest the influence of LCB at branching levels that are undetectable by other methods, including light scattering and intrinsic viscosity.[1] In addition to being sensitive to the presence of LCB, melt rheology is highly sensitive to how branches are distributed among the molecules. To take but one simple example, the rheology of a "star" polymer, with a single branch point, is different from that of a "comb", with many branch points distributed along a single "backbone".

Because of this unrivaled sensitivity, one would like to use the rheological measurements themselves to characterize branching.[1] The use of rheometry as an analytic method to infer molecular information has already been proved successful in the case of polydisperse linear polymers, where the theory of "double reptation"[2−4] allows the linear viscoelastic spectrum to be inverted to obtain the molecular weight distribution.[5−8]

However, implementation of an analogous method of "analytic rheology" for long-chain branched polymers is frustrated by the complexity of the influence of branching on rheology.[9,10] As an example, consider the zero-shear viscosities of polyethylenes, gathered from several literature sources, compiled in Table 1, and plotted in Figure 1, against the weight-average molecular weight M_w.[11−14] The line in this figure is the benchmark line for linear polyethylenes without long side branches at 190 °C, namely[15]

$$\eta_0 = 5.8 \times 10^{-14} M_w^{3.41} \quad \text{at 190 °C} \qquad (1)$$

Polydispersity (without LCB) is thought to produce little or no deviation from eq 1. The open symbols in Figure 1 are data obtained at 190 °C, while the filled symbols

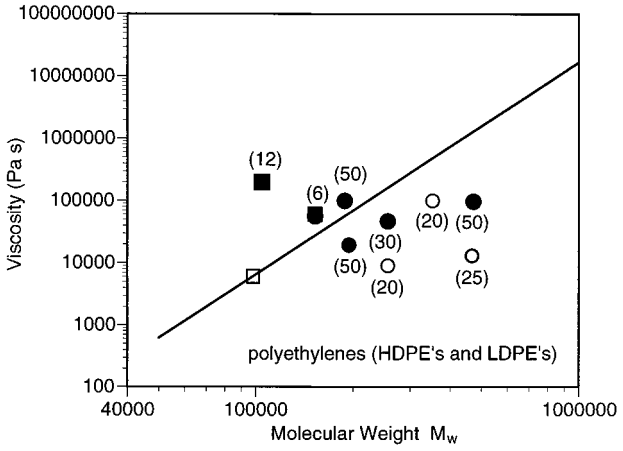

Figure 1. Zero-shear viscosities of polyethylenes from the literature; see Table 1 and the text. The unfilled symbols are data taken at 190 °C and the filled symbols at 150 °C; the data at 150 °C were shifted to 190 °C using an activation energy of 29.29 kJ/mol. The circles are low-density polyethylene (LDPE), and the squares are high-density polyethylene (HDPE). The numbers in parentheses are the "Trouton ratios" at 10 s^{-1}, as discussed in the text. The line is the benchmark line for linear (unbranched) polyethylenes at 150 °C from Arnett and Thomas.[15]

Table 1. Properties of Polyethylenes Plotted in Figure 1

polymer	M_w	M_w/M_n	T (°C)	η_0 (Pa s)	Tr($\dot{\epsilon} = \dot{\gamma} =$ 10 s^{-1})	ref
Dow752 LDPE	194 000	14	150	10^4	50	11
IUPAC A LDPE	472 000	25	150	5×10^4	30	12
"LDPE III"	256 000	10.5	150	2.4×10^4	30	12
"HDPE I"	152 000	13.8	150	2.9×10^4	6	12
"HDPE I"	104 000	5.5	150	10^5	12	14
LDPE	188 000	11.3	150	7×10^4	50	14
"LDPE6"	467 000	25	190	1.3×10^4	25	13
"LDPE9"	256 000	10	190	9×10^3	20	13
"LDPE10"	352 000	20	190	10^5	20	13

are data obtained at 150 °C and shifted to 190 °C. The shifting was performed using an Arrhenius expression with activation energy $E_a = 29.29$ kJ/mol,[15] which is an appropriate activation energy for linear polyethylenes. This yields about a factor of 2 downward shifting of the viscosity. For long-chain branched polyethylenes, E_a can be a factor of 2 or more higher than for linear polymers,[16] and thus the data points at 150 °C have not

10.1021/ma000700o CCC: $20.00
Published on Web 05/25/2001

necessarily been shifted correctly in Figure 1. However, Figure 1 can still be interpreted as a comparison of the data at 150 °C with the linear benchmark line, since if one were to plot both the data and the line at their known viscosities at 150 °C, the relative position of the data with respect to the line would be the same as is shown in Figure 1.

The numbers in parentheses in Figure 1 are the effective "Trouton ratios" for these polymers, each obtained (where available) from the ratio of the uniaxial extensional viscosity $\bar{\eta}_u(\dot{\epsilon})$ to the shear viscosity $\eta(\dot{\gamma})$, at a rate $\dot{\epsilon} = \dot{\gamma} = 10\ s^{-1}$, except where noted otherwise. [The extensional viscosity data were obtained from a variety of sources: from entrance pressure drops using the Cogswell analysis,[11] from the asymptotic stress obtained from a transient extensional rheometer,[12,14] and from Rheotens data.[13] In the case of the data of Wagner et al.,[14] the Trouton viscosity was obtained at $1\ s^{-1}$ because of absence of extensional data at $10\ s^{-1}$. Also, the steady-state shear viscosities for the data of Laun[12] were extracted from the linear viscoelastic data by obtained by applying the "Gleissle mirror rule" that the steady shear viscosity at a given shear rate $\dot{\gamma}$ is equal to the transient linear viscoelastic shear viscosity at a time $t = 1/\dot{\gamma}$ after startup of steady shearing.[17]] The LDPE samples (filled and unfilled circles in Figure 1) contain long branches, while the HDPE samples (filled and unfilled squares) may or may not have long branches, depending on the details of chemical synthesis. Since the viscosities of polyethylenes that are rigorously known to be without long branches lie on the solid line in Figure 1, a deviation from this line is sometimes taken as evidence that the sample in fact contains long branches. High values of the Trouton ratio ($Tr \gg 3$) are also indicative of long-chain branching.

Figure 1 shows that long-chain branching can produce *either an enhancement or a reduction* of the zero-shear viscosity of the polymer relative to a linear polymer of the same weight-average molecular weight. The enhancement or reduction can be very large, as much as 2 orders of magnitude in either direction. The ability of LCB to either enhance or reduce the viscosity of a melt relative to that of a linear polymer of equal molecular mass has been noted before.[1,18,19] This complex nonmonotonic behavior illustrates the extreme difficulty of extracting long-chain branching information from rheological data, especially shear data, which is the most easily obtained.

Nevertheless, recently Janzen and Colby[1] have presented an intriguing semiempirical method for determining the level of long-chain branching almost entirely from zero-shear viscosity alone. The method relies on a formula (eq 2 of Janzen and Colby, ref 1) relating the zero-shear viscosity η_0 to the weight-average molecular weight M_w and a "branching exponent" s/γ, which was obtained by making empirical adjustments to a theory developed for the rheology of fractal gelation clusters near the critical gel point.[20] Janzen and Colby[1] showed that their equation allows one to infer the degree of branching from the zero-shear viscosities of polyethylenes into which long-chain branches were introduced by treatment with known small amounts of peroxides, where each peroxide molecule was assumed to produce a single branch point.

The predictions of the Janzen−Colby equation are presented in Figure 2 for polyethylenes with fixed weight-average molecular weight of 200 000 and a

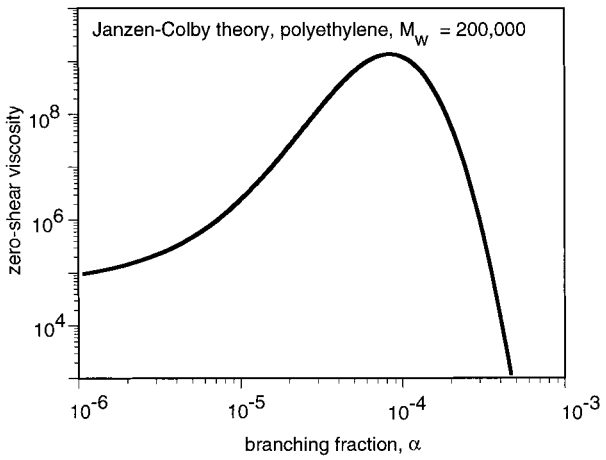

Figure 2. Prediction of the zero-shear viscosity η_0 from the theory of Janzen and Colby[1] for "randomly branched" polyethylene, as a function of the fraction of carbons that are branch points for samples with weight-average molecular weight 200 000.

varying degree of branching α, where α is the fraction of total carbons that are long-branch vertexes. (The parameters for the calculations for polyethylene are given in Table 1 of Janzen and Colby.) Note that the zero-shear viscosity is enormously sensitive to branch content, even at fixed weight-average molecular weight, and that the dependence of η_0 on branching fraction α is *nonmonotonic*. For a linear polyethylene ($\alpha = 0$) with $M_w = 200\ 000$, η_0 is 69 000 Pa s, as given by eq 1. As α increases, η_0 is predicted to *increase* 4 orders of magnitude to 10^9 Pa s at $\alpha \approx 10^{-4}$ and then to *decrease* precipitously to values lower than that of a linear polymer when α exceeds 3×10^{-4}.

In principle, if the weight-average molecular weight of the polymer is known *and if the polymer is described by the random-branching model of Janzen and Colby*, one could infer the branching level α from the zero-shear viscosity, provided that one could determine independently that α is either higher or lower than that at which η_0 goes through a maximum, so that one could decide between the two values of α that are possible for each value of η_0.

While the formulas of Janzen and Colby have been successfully applied to the predictions of branching level in randomly cross-linked melts of linear chains, the applicability of the approach to other branched melts, such as those of Figure 1, is uncertain. We therefore wish to explore the degree to which predictions such as that shown in Figure 2 are sensitive to the *type* of branching present and whether it might be possible to infer branching type from linear viscoelastic data.

Fortunately, recent advances in polymer molecular theory, most notably by McLeish, Milner, and coworkers,[10,21−23] now permit accurate, even quantitative, predictions to be made, not only of the zero-shear viscosity η_0 but also of the entire frequency-dependent linear viscoelastic response, of well-characterized model branched samples such as monodisperse stars, "H" molecules, and even bidisperse stars or stars mixed with linear molecules. However, to use these advances to solve the general problem of branched-polymer characterization, such theories must be generalized so that mixed systems can be considered that are not only polydisperse in molecular mass but also polydisperse in branch length and branch placement. In what follows, we develop a general model for the linear viscoelasticity

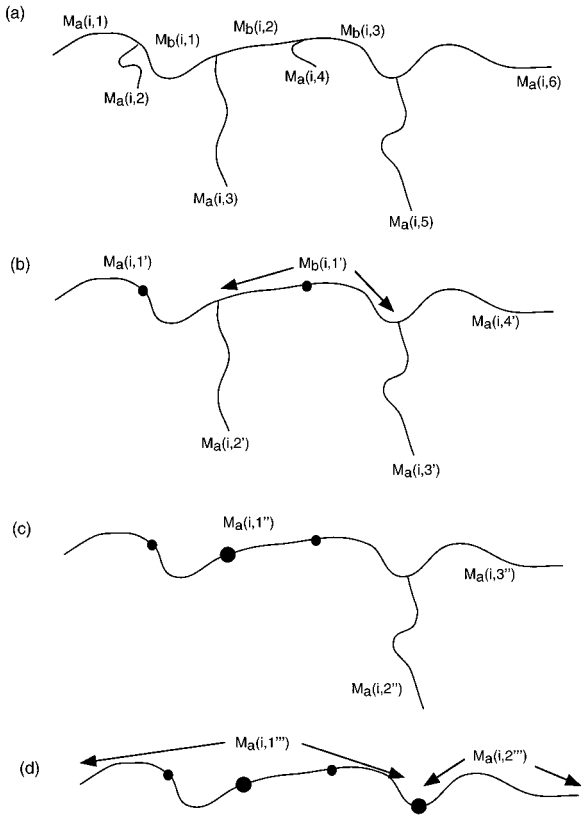

Figure 3. Conceptualization of algorithm for computing hierarchical relaxation of an arbitrary comb-branched polymer, illustrated in (a). The molecule consists of arms and backbone segments. Initially, only the arms can move, initially by primitive path fluctuations, from the arm tips inward. When an arm fully relaxes, it is pruned away and replaced by a "bead" at the branch point to represent the frictional drag contributed by that arm. After the arm and backbone segment to which the pruned arm were attached are merged, the arms and backbones are renumbered; see (b). The drag produced by a "bead" is accounted for by a pause in the relaxation of the arm on which it resides. Continued arm relaxation converts the molecule into a star (c) and finally a linear chain (d). The linear chain can complete its relaxation by reptation.

of such arbitrarily branched melts. We then both test the model against available experimental data for model branched and unbranched polybutadiene melts and use the model to assess the prospects for using rheology as a general characterization tool for branched melts.

II. Melt Specification and Model Overview

A typical commercial branched polymer melt is composed of multiple species of linear, star, and comb molecules containing backbones and branches that are polydisperse in length. Here, we propose a computational algorithm for calculating the viscoelastic response of such systems. For the present, we allow our melt to contain linear, star, and comb molecules but no higher-order branched structures in which branches themselves have branches. (The scheme could, however, be generalized to consider branches on branches, but this is beyond the scope of the present work.) The most general molecule we consider has the structure shown in Figure 3a; it is a comb in which the functionality of each branch point is 3. Our melt is composed of an arbitrary mixture of such molecules. Molecule "i" has $n_a(i)$ arms; arm j of molecule i has a molecular weight of $M_a(i,j)$. Portions of the molecule between branch points are backbone segments. There are $n_a(i) - 3$ backbone segments, with

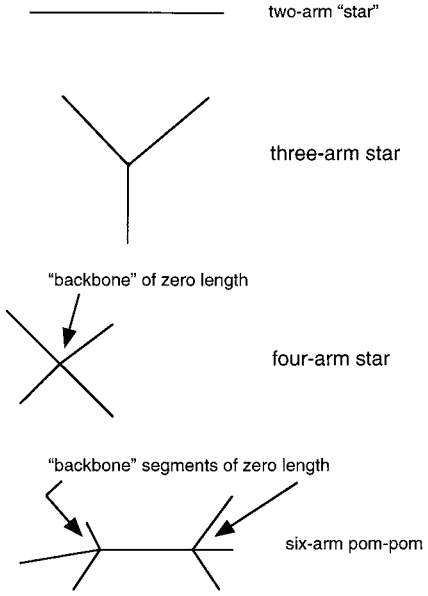

Figure 4. Linear, star, and pom-pom molecules can be obtained as special cases of "comb" molecules that contain only two arms (linear), three arms (3-arm star), four arms with a zero-length backbone (4-arm star), or six arms with three backbone segments, two of zero length (six-arm pom-pom).

molecular weights $M_b(i,j)$, with $j = 1, 2, \ldots, n_a(i) - 3$. The total molecular weight of the ith molecule is therefore

$$M(i) = \sum_{j=1}^{n_a(i)} M_a(i,j) + \sum_{j=1}^{n_a(i)-3} M_b(i,j) \qquad (2)$$

A three-arm star is a special case of this structure obtained when $n_a = 3$. A four-arm star can be obtained as a comb with two branch points and a backbone molecular weight of zero; see Figure 4. Likewise, stars with any number of arms can be constructed as multi-arm combs with backbone segments of zero length. We can also construct the six-arm "pom-pom" molecule shown in Figure 4 by including one long backbone segment and two zero-length backbone segments. The "H" molecule is a special case of a pom-pom with only four arms, two at each end, and with no zero-length backbone segments. A linear molecule is obtained if there are fewer than three branches. For some purposes, as described later, it will be useful for us to consider a linear molecule to be a "two-arm star".

The melt to be considered is composed of an arbitrary mixture of such molecules, each having its own volume (or mass) fraction ϕ_i and each having a potentially different distribution of arm lengths and arm positions. The volume fractions of arm and backbone segments for molecule i are therefore

$$\phi_a(i,j) = \phi_i \frac{M_a(i,j)}{M_i}; \quad \phi_b(i,j) = \phi_i \frac{M_b(i,j)}{M_i} \qquad (3)$$

As envisioned by McLeish,[9] the molecule depicted in Figure 3 relaxes *hierarchically* from its extremities inward. Thus, the backbone segments are initially "frozen" and can only relax after at least one end of the backbone is released by complete relaxation of one or more arms. The time required for an arm to relax is controlled by the molecular weight of that arm and by the "dynamic dilution" produced by the relaxation of the

surrounding molecules with which the arm is entangled. At times long after an arm has completely relaxed, the arm no longer imposes topological restrictions on surrounding molecules and acts only as a "frictional" element within the molecule to which it is attached, where its friction is proportional to the arm relaxation time. (A scheme for hierarchical relaxation in multiply branched polymers was developed earlier by McLeish[9] to analyze the viscoelasticity of regular treelike branched polymers. Our scheme will apply to irregularly branched molecules, but ones which (for now) have only a single level of branching, i.e., no branches on branches.)

The relaxation of the molecule shown in Figure 3 can be broken into a series of stages shown in Figure 3a−d. First, the shorter arms relax completely and are converted to frictional "beads" which bog down motion of the rest of the molecule but are otherwise effectively nonexistent at the time scale of Figure 3b. In Figure 3b, two such arms have been converted to "beads", as shown by the dark dots replacing the branch points. The loss of these arms lengthens one of the arms by adding to it a backbone segment, while the loss of the other arm merges two other backbone segments together. Thus, in Figure 3b, there remain only four arms and only one backbone segment, and so we renumber the arms and backbone as shown and place primes on their branch indices. The remaining backbone segment is still immobile, while arm 1′ in Figure 3b is a longer arm than was arm 1 in Figure 3a, and is also slowed by the frictional bead representing the lost arm. As time progresses, arm 2′ relaxes completely and is replaced by a frictional bead in Figure 3c, represented by a large dot to illustrate the rather large drag produced by the long arm 2′ that has been lost. Now, there are only three arms, and the molecule has become a three-arm star, with a very long arm 1″, which contains three frictional beads representing lost arms. Next, arm 2″ relaxes, so that in Figure 3d, there are only two "arms" left, and four frictional beads representing lost arms. At this point, we can consider the molecule to be a "two-arm star", or it can be considered to be a linear molecule. We shall choose between these two options by comparing the reptation time of the linear molecule with the present time t. As long as the reptation time is longer than the present time t, we shall treat the molecule as a "two-arm star", whose relaxation is dominated by fluctuations of the ends. Once the repation time is exceeded, the molecule relaxes quickly and entirely by reptation.

If the mass fraction of molecule i is ϕ_i, then only a portion of this mass, $\Phi_i(t)$, is unrelaxed at time t. Thus, $\Phi_i(t) = \phi_i$ at $t = 0$, and $\Phi_i(t) < \phi_i$ thereafter. The total unrelaxed mass fraction contributed by all components is $\Phi(t) = \sum_i \Phi_i(t)$. It is this unrelaxed portion that topologically constrains surrounding molecules.

III. The Relaxation Algorithm

A. Relaxation by Arm Fluctuation. On the basis of this viewpoint, we define the following algorithm for relaxation of an arbitrary blend of linear, star, and comb molecules. We consider the case of linear viscoelastic relaxation after a small "step" strain imposed at time $t = 0$, for which we will compute the linear viscoelastic modulus $G(t)$. We regard all polymer molecules in the melt as "combs"; stars are "combs" with no backbone, and linear molecules are "combs" having no backbone and two equal-length arms. Backbone material is immobile, and each arm relaxes initially by primitive-path fluctuations. We shall initially describe the relaxation of the arms without considering the constraint-release process; that is, for the moment, we will pretend that $\Phi = 1$. In this case, the relaxation time of a portion of an arm follows[24]

$$\tau_a(i,j,\xi(i,j)) = \tau_0 S_a^{3/2}(i,j) \exp[\nu S_a(i,j)\, \xi^2(i,j)] \quad (4)$$

where $S_a(i,j) \equiv M_a(i,j)/M_e$, with M_e the entanglement spacing and $\nu = 15/8$ is a constant. $\xi(i,j)$ is an arm coordinate that runs from zero to unity as one moves along the contour of the arm from the free end to the branch point. The prefactor of this exponential, $\tau_0 S_a^{3/2}(i,j)$, is related to the frictional drag coefficient that controls the rate at which fluctuations are attempted, while the exponential is due to the entropic barrier to deep fluctuations. This prefactor ignores a mechanism for much faster relaxation of branch tips by "early-time" shallow fluctuations described by Milner and McLeish.[22,23]

At any time t, the (i,j) arm will have relaxed from its free end to a point $\xi(i,j)$ obtained by equating $\tau_a(i,j,\xi(i,j))$ with t; hence

$$t = \tau_0 S_a^{3/2}(i,j) \exp[\nu S_a(i,j)\, \xi^2(i,j)] \quad (5)$$

Taking the logarithm of both sides of eq 5 and defining $x \equiv \ln(t)$ gives

$$x = \ln(\tau_0 S_a^{3/2}(i,j)) + \nu S_a(i,j)\, \xi^2(i,j) \quad (6)$$

As logarithmic time (x) increases, more of the (i,j) arm relaxes, and $\xi(i,j)$ increases; the incremental increase in $\xi(i,j)$ is related to the incremental increase in x through a differential form of eq 6:

$$dx = 2\nu S_a(i,j)\, \xi(i,j)\, d\xi(i,j) \quad (7)$$

B. Dynamic Dilution. So far, we have not included the influence of relaxation of "matrix" chains on the rate of relaxation of the (i,j) arm. According to the "dynamic dilution" concept of Ball and McLeish,[21] the effect of matrix-chain relaxation is accounted for by replacing the undiluted arm entanglement density S_a by the diluted density ΦS_a in eq 7:

$$dx = 2\nu\Phi(t)\, S_a(i,j)\, \xi(i,j)\, d\xi(i,j) \quad (8)$$

This is the *Ball−McLeish equation*. At any instant in time after a small step strain, $\Phi(t)$ is the total fraction of matrix material that remains unrelaxed. It is obtained by adding up the unrelaxed parts of all arms and the backbones:

$$\Phi(t) = \sum_i [\sum_{j=1}^{n_a(i)} \phi_a(i,j)(1 - \xi(i,j,t)) + \sum_{j=1}^{n_b(i)} \phi_b(i,j)] \quad (9)$$

The dynamic dilution factor $\Phi(t)$ in eq 8 couples the relaxation of each arm (i,j) to the relaxation of every other polymer arm. We can now rewrite eq 8 as

$$d[\xi^2(i,j)] = \frac{dx}{\nu\Phi(t)\, S_a(i,j)} \quad (10)$$

where we have replaced $d\xi(i,j)\, \xi(i,j)$ with $^1/_2 d[\xi^2(i,j)]$, so that $\xi(i,j)$, which can be zero, does not appear in the denominator of eq 10. In this form, the Ball−McLeish

equation tells us how much of each arm relaxes in a given small increment dx of logarithmic time. Combined with eq 9, eq 10 is the basis for a general time-integration algorithm for tracking the relaxation of polymer arms in an arbitrary mixture of branched polymers.

C. Prefactors and Arm-Specific Initial Conditions. Note, however, in eq 5, that each arm has a different prefactor, $\tau_0 S_a^{3/2}(i,j)$, which does not appear in the differential dependence of d$\xi(i,j)$ on dx in eqs 8 and 10. According to eq 6, the different prefactors are manifested as different *initial conditions* of the dependence of $\xi(i,j,t)$ on x; thus, a given $\xi(i,j,t)$ should remain at zero until x reaches the value $\ln(\tau_0 S_a^{3/2}(i,j))$ for arm (i,j). So, the various prefactors can be accounted for by holding each $\xi(i,j)$ fixed at the initial value $\xi(i,j) = 0$ until x reaches a value $x_0(i,j)$ given by

$$x_0(i,j) = \ln(\tau_0 S_a^{3/2}(i,j)) \tag{11}$$

Each arm (i,j) therefore begins its fluctuation relaxation process at a different logarithmic time $x_0(i,j)$, and once it starts relaxing, its relaxation obeys eq 10. By converting the differential increments d$\xi^2(i,j)$ and dx into small, but finite, increments, we can then write a simple explicit Euler integration algorithm for the relaxation of an arbitrary mixture of arms of various molecular masses $M_a(i,j)$.

D. Arm Collapse and Waiting Times. This algorithm can be carried forward until a time is reached at which an arm becomes completely relaxed. For example, say $\xi(i^*,j^*)$ reaches unity at some time t^* for arm (i^*,j^*). At this point, we replace the arm by a frictional "bead" along the arm or backbone segment to which the newly relaxed arm is attached; see Figure 3b. If the arm collapses onto a backbone segment, like branch 4 in Figure 3a, the bead can be temporarily ignored, since the backbone is immobile, until one of the constraining branch points is released. If the arm collapses onto another arm, such as arm 2 in Figure 3a, we form a new arm, arm 1′, whose length is increased over that of the old arm 1 by the addition of backbone segment 1. Thus,

$$S_a(i,1') = S_a(i,1) + S_b(i,1) \tag{12}$$

The contour variable $\xi(i,1')$ must also be rescaled to include the additional length of unrelaxed polymer from the backbone segment $(i,1)$:

$$\xi(i,1',t^*) = \frac{\xi(i,1,t^*)\, M_a(i,1)}{M_a(i,1) + M_b(i,1)} \tag{13}$$

Now we need to consider the relaxation of this new "compound arm", 1′, which consists of arms 1 and 2 plus backbone segment 1. The motion of this compound arm is bogged down by the drag from the collapsed pendant arm 2. The relaxation of the compound arm 1′ will, in general, depend on the length and location of the attached pendant arm 2. For example, if the pendant arm 2 is almost as long as arm 1, then we expect the branch point to remain rather immobile until arm 1 relaxes nearly to the branch point. Thereafter, the backbone segment 1 can begin to relax, but only more slowly, because the relaxation of this backbone segment requires motion of the branch point, which is sluggish because of the two attached branches 1 and 2. On the other hand, if arm 2 is much shorter than arm 1, we expect significant branch point motion to begin before arm 1 has completely relaxed.

Hence, the distribution of fluctuation times $\tau_a(i,1',\xi(i,1'))$ for the compound arm 1′ will, in general, be quite different from that of a simple arm of equal length $S_a(i,1')$. The relaxation behavior will be even more complex for arms with more than one pendant arm, such as arm 1″ in Figure 3c. Given the complexity of the problem, a general solution for the relaxation of compound arms is not yet available. In addition, data for branched polymers with controlled, unequal, arm lengths, or controlled arm spacings, are not yet available in the literature, so any theory, were it available, could not yet be adequately tested. We note that the effect of pendant arms on the fluctuation of an arm to which they are attached is expected to be much more complicated due to the effect of pendant arms on the reptation of an otherwise linear chain. This is because reptation is a uniform motion of the whole backbone, and so a pendant arm will exert the same drag on its environment, no matter where it is attached along the reptating chain. Fluctuations, on the other hand, usually involve non-uniform chain motion and so are affected differently, depending on where the pendant arm is attached.

Given these complications and uncertainties, we will for the time being adapt a simple, naive method for computing the relaxation of a compound arm, a method that treats the pendant arm as a simple source of drag that slows fluctuations of the compound arm at times longer than the relaxation time of the pendant arm. We will test the predictions of this method against experimental rheology data for pom-pom and comb molecules. We will also examine the sensitivity of these predictions to our model of branch-point flucutations by turning off branch-point fluctuations altogether, while still allowing reptation of the backbone. We recognize the inadequacy of our model of branch-point motion and hope that future theoretical and experimental work will provide a basis for an improved approach.

To develop our algorithm for branch-point fluctuations, first recall that, at the time t^*, the tube coordinate for the compound arm is set to the value $\xi(i,1',t^*)$ given by eq 13. For times $t > t^*$, we assume that the relaxation of the compound arm 1′ is affected by the drag produced by the pendant arm 2. To account for this, we take advantage of the hierarchical character of the relaxation process and the generality of the Ball−McLeish eq 10. That is, we stop integrating eq 10 and restart integration with a different initial condition, one dictated by the relaxation time at the point at which the fluctuation process resumes after the collapse of arm 2. To understand this, suppose arm 2 were absent, and so no arm collapse occurs at time t^*. Nevertheless, at this time t^*, we could stop the integration of eq 10 and immediately restart it with the new, nonzero initial condition

$$\xi(i,1,t) = \xi(i,1,t^*) \quad \text{at } x = \ln(t) = x^* \tag{14}$$

This sudden stop-and-restart of integration has no effect on the result but simply emphasizes the fact that at any point in the integration we can stop and restart the integration, using as initial condition the stopping point of the previous integration. However, in reality, at time t^*, the drag on the new arm 1′ is suddenly increased, and this must increase the effective prefactor for the arm fluctuation process. This increase in prefactor means that the time at which the new integration is

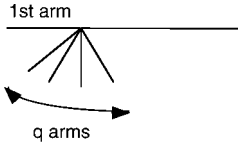

Figure 5. Clump of $q + 1$ equal-length arms, which produces a drag proportional to the number of arms $q + 1$.

restarted must be adjusted; i.e., there must be a delay in restarting the integration. We compute this delay by noting that by definition the relaxation time of the collapsed arm $\tau_a(i,2)$ is equal to the time t^* at which the collapse occurs. In addition, we remind ourselves that the relaxation process is hierarchical; the relaxation time of a newly relaxing portion of the molecule is just a product of the relaxation time of a previously relaxed portion (which is the new frictional "prefactor" t^*) times a factor that accounts for the slowing down of the relaxation process. When arm 2 collapses, the frictional drag contributed by this collapsed arm corresponds to a prefactor t^*, identical to the prefactor for arm 1 that we would use to restart the integration at time t^* if arm 2 were not present. Thus, the prefactor we really should use is $2t^*$, to account for the doubling of the frictional drag at time t^*. So, rather than immediately restarting the integration, the restart condition is

$$\xi(i,1',t) = \xi(i,1',t^*) \quad \text{at } x = \ln(2t^*) = \ln(t^*) + \ln(2) \quad (15)$$

Hence, the collapse of arm 2 leads to a logarithmic delay in relaxation of arm 1′ of $\Delta x = \ln(2)$. Generalizing, we obtain the rule that *at each collapse of an arm into another arm, there is a pause of* ln(2) *in x, before relaxation of the new elongated arm can begin*.

If, at a later time t^{**} *during the pause in relaxation of arm 1′* there is collapse of another arm onto arm 1′, then additional drag must be added to arm 1′, which extends the duration of the pause. If the first pause still has an interval Δx^* left to run when the next arm collapses, then the first pause would have come to an end at time $t = t^{**} \exp(\Delta x^*)$, if it were not for the collapse of the next arm. Using the same argument we used earlier, the collapse of the next arm should add to the drag and hence augment the pause by an additional time t^{**}. Hence, the extended pause will come to an end at time t^{**} $(\exp(\Delta x^*) + 1)$ The logarithmic pause is therefore increased at time t^{**} from Δx^* to a new value Δx^{**} given by

$$\Delta x^{**} = \ln[\exp(\Delta x^*) + 1] \quad (16)$$

Note that if q arms collapse onto the same arm one after another in rapid succession (i.e., virtually simultaneously), then the logarithmic pause in relaxation after the first arm collapses is ln(2); this is augmented to $\ln[\exp(\ln(2)) + 1] = \ln(3)$ after the second, and so on, until, relaxation of all q arms produces a total logarithmic pause of $\ln(q + 1)$. This implies that the clump of $q + 1$ arms shown in Figure 5 will act at long times like a single "bead" whose drag corresponds to a relaxation time of $(q + 1)\tau_a$, where τ_a is the relaxation time of just one of these arms.

With this rule, the integration of eq 10 can continue. With each collapse of an arm, the collapsed arm is discarded, and the remaining ones are renumbered. Each time an arm collapses, we note its relaxation time τ_a, which is just the time t at which the collapse occurred, and keep a running sum, $\tau_{a,tot}(i)$, of the total relaxation times of all the collapsed arms. We shall need this running sum in what follows.

We also keep track of the total drag coefficient that must be associated with each remaining backbone segment. We store this drag in the form of an equivalent time constant $\tau_{b,tot}(i,j)$. If the backbone segment has no beads representing collapsed arms attached to it, we take $\tau_{b,tot}(i,j) = \tau_0 S_b^{3/2}(i,j)$. As arms collapse into the backbone, thus merging two backbone segments, say segments j and $j + 1$, into a new segment j', we reset $\tau_{b,tot}$ by adding together the drag of the two backbones and the arm:

$$\tau_{b,tot}(i,j') = \tau_{b,tot}(i,j) + \tau_{b,tot}(i,j+1) + t^* \quad (17)$$

where t^* is the time at which the two backbone segments merged and is therefore also the relaxation time of the arm whose collapse precipitated the merger.

As long as the backbone segment remains in the backbone, and is not merged into one of the terminal arms, this time constant $\tau_{b,tot}(i,j)$ plays no role. But once the backbone segment merges with a terminal arm (such as the merger that occurs in Figure 3b,c, where backbone 1′ merges with arm 1′), its drag must be added to that of the arm. When this merger occurs, we combine the backbone time $\tau_{b,tot}(i,1')$ with the prefactor for arm 1′, i.e.,

$$x_0(i,1'') = \ln[\exp(x_0(i,1')) + \tau_{b,tot}(i,1')] \quad (18)$$

If this new prefactor is less than the current log time x, then we take a pause of ln(2), as usual. If $x_0(i,1'') > x$, the logarithmic pause Δx^{**} is given by eq 16 with $\Delta x^* = x_0(i,1'') - x$.

When only three arms are left, the molecule has become a three-arm star. When one of the remaining three arms disappears, the drag associated with that arm can be assigned to either of the two remaining arms; we choose to assign it to the arm that has relaxed to the greater extent, i.e., the arm with the larger value of ξ.

E. The End Game: Reptation. With only two arms left, the molecule is effectively linear, as shown in Figure 3d. We must therefore consider the possibility that the chain will complete its relaxation by reptation, rather than by arm fluctuations. Of course, the chain may have started out as a linear chain, in which case we would represent it as a "2-arm star", with each arm of equal length, but we would soon need to consider the possibility that this molecule completes its relaxation by reptation, rather than by fluctuations of the two arms. To consider reptation, we estimate the reptation time of the linear molecule or backbone into which the chain has collapsed by the formula

$$\tau_d(i) = \frac{a^2 (S_b'(i))^2 \Phi(\tau_{repstep}(i)) \zeta_{tot}(i)}{\pi^2 k_B T} \quad (19)$$

where a is the undiluted reptation tube diameter, S_b' is the number of remaining undiluted entanglements in the chain that have not yet been relaxed by primitive-path fluctuations, and ζ_{tot} is the total drag coefficient for reptative motion of the molecule. The dilution factor Φ is evaluated at the time $\tau_{repstep}(i)$ required for chain i to reptate one tube diameter (see below).

To obtain eq 19, we have used eq 6.19 in Doi and Edwards,[25] which can be written as

$$\tau_d = \frac{1}{\pi^2}\frac{a^2 S_b{}^2 \zeta_{tot}}{k_B T} \tag{20}$$

where we note that Nb^2 in Doi and Edwards's expression is the mean-square end-to-end separation of the chain (where N is the number of monomers in the chain and b the statistical segment length of a monomer); Nb^2 is therefore also equal to $S_b a^2$. The total drag coefficient for the chain is $N\zeta = \zeta_{tot}$. To obtain eq 19, we replace the entanglement spacing a in the Doi−Edwards expression with the diluted spacing $a[\Phi(\tau_{repstep}(i)]^{1/2}$. We also account for the portions of reptation "tube" that have already been lost due to fluctuations; that is, we replace S_b by $S_b'(i)$, where

$$S_b'(i) = S_a(i,1)(1 - \xi(i,1,t)) + S_a(i,2)(1 - \xi(i,2,t)) \tag{21}$$

The total drag coefficient $\zeta_{tot}(i)$ in eq 19 has contributions from the backbone of the molecule plus all the arms that have been collapsed into the backbone. Each collapsed arm contributes a drag coefficient $\zeta_a(i,j)$ that can be obtained from the relaxation time of that arm via the fluctuation−dissipation relationship between friction and diffusivity combined with the relationship between diffusivity and relaxation time:[26]

$$\zeta_a(i,j) = \frac{2k_B T \tau_a(i,j)}{a^2} \tag{22}$$

Thus, the running sum over arm relaxation times $\tau_{a,tot}(i) = \sum_j \tau_a(i,j)$ (mentioned at the end of section III.D) contributes to the drag coefficient the quantity:

$$\zeta_{a,tot}(i) = \frac{2k_B T \tau_{a,tot}(i)}{a^2} \tag{23}$$

The drag coefficient due to the backbone can be computed from the Rouse time for relaxation of a single undiluted entanglement, which is the so-called "equilibration time" τ_e given by eq 6.18 of Doi and Edwards[25] with $Nb^2 = a^2$ and $\zeta N = \zeta_{tot}$. From this, we obtain the contribution of the backbone to the drag:

$$\zeta_{b,tot}(i) = N\zeta = 3\pi^2 \frac{k_B T}{a^2} S_b(i)\tau_e \tag{24}$$

where

$$S_b(i) = S_a(i,1) + S_a(i,2) \tag{25}$$

is the total undiluted number of entanglements in the backbone, i.e., in the effectively linear molecule that remains after all but two arms have relaxed.

Combining eqs 19, 20, 23, 24, and 25 and taking $\zeta_{tot}(i) = \zeta_{a,tot}(i) + \zeta_{b,tot}(i)$ gives

$$\tau_d(i) = \frac{2}{\pi^2}(S_b'(i))^2 \Phi(\tau_{repstep}(i))\left[\frac{3\pi^2}{2}\tau_e S_b(i) + \tau_{a,tot}(i)\right] \tag{26}$$

Φ in eq 26 is evaluated not at the present time t, but at the time $\tau_{repstep}(i)$ required for the chain to reptate one tube diameter, since it is in the tube defined at $\tau_{repstep}$ that the chain must reptate. We take this time $\tau_{repstep}$ to be

$$\tau_{repstep}(i) = \frac{3\pi^2}{2}\tau_e S_b(i) + \tau_{a,tot}(i)$$

We note that while eq 26 is the simplest formula for τ_d, McLeish et al.[10] have presented a formula with additional prefactors (their eq 12) associated with a factor of $^5/_4$ introduced in the definition of the tube diameter, a factor of 6 multiplying $\tau_{a,tot}$ that McLeish et al. believe leads to a better description of the drag on a branch point and a power other than unity to which the dilution factor Φ is raised. These innovations partially cancel and in any event have not been thoroughly tested by comparisons with data for multiple polymer samples. Since we wish to introduce our model in the simplest way possible, we shall ignore these factors here, except for the remark that further theoretical work as well as detailed comparisons with experiments will be needed to completely settle on an appropriate choice of prefactors.

With the estimate of the reptation time given in eq 26, we can now determine whether reptation occurs at a given point in the relaxation process by comparing τ_d with t, the present time. If $\tau_d > t$, the chain is not yet ready to relax by reptation, and we should continue to regard the chain as a "two-arm star" that relaxes by primitive-path fluctuations of the two ends. However, as these fluctuations continue, $\xi(i,1,t)$ and $\xi(i,2,t)$ increase, and hence $S_b(i)$ and therefore $\tau_d(i)$ decrease, while t, of course, increases. Eventually, t exceeds $\tau_d(i)$, and chain i then relaxes completely by reptation. It may happen that one of the two arms relaxes completely before t exceeds $\tau_d(i)$. In that case, the chain becomes a "one-arm star" in which $S_b'(i) = S_a(i,1)(1 - \xi(i,1))$ and $S_b(i) = S_a(i,1)$, and fluctuation relaxation of that one arm continues until it is overtaken by reptation or until that last arm relaxes completely by fluctuations.

We also note that when the chain has been reduced to a "two-arm" star, the lengths of the two arms that remain depend on the order in which the original arms have collapsed. In the singular case in which all original arms are identical in length, the algorithm arbitrarily relaxes the arms in order from one end of the backbone to the other, and for a many-arm comb, the "two-arm" star that remains after all but the final two arms have collapsed is "lop-sided," in that one of the remaining arms is very much longer than the other. Even a slight polydispersity in arm length breaks the degeneracy, however, and if the various arm lengths are randomly distributed along the backbone, then the final "two-arm" star will in most cases be much less lop-sided.

F. Constraint-Release Rouse Motion—The Supertube Fraction. Now when $t > \tau_d$, the remaining unrelaxed portion of the chain relaxes "suddenly", and the molecule can be removed and the remaining chains renumbered. In addition, the unrelaxed volume fraction Φ is suddenly decreased to account for the loss of the chain. Since this decrease in Φ is "sudden" (really it decreases via an exponential decay which we approximate here as a step), one cannot assume that the tube diameter governing the relaxation of other chains increases as fast as Φ decreases. That is, chains that see a sudden decrease in their entanglement mesh density explore their new, larger tubes only gradually,

by a process of "constraint-release Rouse" motion. When "constraint-release Rouse" processes are initiated, the dynamic dilution formula, eq 10, no longer applies. Instead, the volume fraction of mesh chains that act as effective constraints is no longer Φ, the unrelaxed fraction, but a higher fraction Φ_{ST}, the volume fraction defining the portion of a "supertube" that the chain is actually able to explore in the allowed time. A discussion of "supertube" relaxation is beyond the scope of this work but is described in detail in Viovy et al.[27] and Watanabe.[28] For our purposes, we only need the formula from Milner et al.[29] that describes the Rouse relaxation of the supertube volume fraction, namely

$$\Phi_{ST} = \Phi_{ST,0}\left(\frac{t}{t_0}\right)^{-1/2} \tag{27}$$

where t_0 is the time at which supertube relaxation is activated and $\Phi_{ST,0} = \Phi(t_0^-)$ is the volume fraction of unrelaxed material just before the sudden relaxation by reptation occurs. Thus, at time t_0, Φ drops suddenly from $\Phi(t_0^-)$ to a smaller value $\Phi(t_0^+)$, while Φ_{ST} begins a gradual decrease from $\Phi_{ST}(t_0) = \Phi(t_0^-)$ to smaller values, following eq 27. During supertube relaxation, the fraction of remaining entanglements used in eqs 10 and 26 must be taken as $\Phi_{ST}(t)$ rather than Φ. Thus, we replace eqs 10 and 26 by

$$\mathrm{d}[\xi^2(i,j)] = \frac{\mathrm{d}x}{\nu\Phi_{ST}(t)\, S_a(i,j)} \tag{12'}$$

$$\tau_d(i) = \frac{2}{\pi^2}(S_b'(i))^2\Phi_{ST}(\tau_{repstep}(i))\left[\frac{3\pi^2}{2}\tau_e S_b(i) + \tau_{a,tot}(i)\right] \tag{26'}$$

Eventually, if $\Phi_{ST}(t)$ drops below $\Phi(t)$, constraint-release Rouse relaxation ceases, and $\Phi_{ST}(t)$ can again be taken to be identical to $\Phi(t)$, until another sudden relaxation occurs.

For the case of long polymers for which fluctuations are negligible, eq 26′ reduces to $\tau_d(i) = 3\tau_e(S_b(i))^3$, in agreement with the formula for the relaxation time used in "double reptation" (discussed in the Introduction).

G. "Disentanglement" Relaxation. For completeness, we discuss one last relaxation process, namely "disentanglement," which is most likely to occur if short chains are part of the polymer mixture. Disentanglement occurs when the density of surviving entanglements $S_a(i,j)\Phi_{ST}$ for some arm (i,j) falls below the entanglement threshold; i.e., $S_a(i,j)\Phi_{ST}$ drops to a value around unity. If this occurs, then we assume that the remainder of the arm suddenly relaxes and initiate a supertube relaxation process. Here we shall take $S_a(i,j)\Phi_{ST} = S_{a,min} = 1$ as the threshold for disentanglement. Disentanglement is not important in the results that are reported here.

H. Formulas for the Relaxation Moduli. The above discussion completes the description of chain relaxation in a general mixture of branched and linear polymers. We now need to write down the expression for the stress, which, in the linear viscoelastic limit considered here, reduces to the time-dependent modulus. For relaxation processes that include constraint release by either dynamic dilution or supertube relaxation, the general expression for the time-dependent modulus is

$$G(t)/G_N^0 = \int_{t_i}^{t_f}\exp(-t/t')\,\Phi_{ST}(t')\,\frac{\mathrm{d}\Phi(t')}{\mathrm{d}t'}\,\mathrm{d}t' + \int_{t_i}^{t_f}\exp(-t/t')\Phi(t')\,\frac{\mathrm{d}\Phi_{ST}(t')}{\mathrm{d}t'}\,\mathrm{d}t' \tag{28}$$

where G_N^0 is the plateau modulus for the polymer, and $\Phi(t')$ and $\Phi_{ST}(t')$ are the unrelaxed fraction and the supertube fraction at time t' during the relaxation process. The times t_i and t_f are the initial and final times of the simulations. Since whatever relaxes at time t' during the simulation is assumed to have a relaxation time t', the exponentials in eq 23 give the relative contributions to the modulus at time t of the material with a relaxation time of t'. Equation 28 can be rearranged to

$$G(t)/G_N^0 = \int_0^1\exp(-t/t')\,\Phi_{ST}(t')\,\mathrm{d}\Phi(t') + \int_0^1\exp(-t/t')\,\Phi(t')\,\mathrm{d}\Phi_{ST}(t') \tag{29}$$

Thus, eq 29 can be integrated by simply summing over the increments in Φ and Φ_{ST} using values of Φ and Φ_{ST} obtained at the logarithmic time steps used in the relaxation algorithm.

In the limit where there is no supertube relaxation, $\Phi_{ST} = \Phi$, and eq 29 reduces to

$$G(t)/G_N^0 = 2\int_0^1\exp(-t/t')\,\Phi(t')\,\mathrm{d}\Phi(t') = \int_0^1\exp(-t/t')\,\mathrm{d}(\Phi^2(t')) \tag{30}$$

Equation 30 is the famous result for "double reptation" that the unrelaxed portion of the entanglement network contributes to the modulus in proportion to the square of the remaining fraction of entanglements.[2-4] When supertube relaxation is occurring, there is a loss of modulus both due to continuing relaxation of entangled chains, and therefore due to a decrease in Φ (the first term on the right of eq 29), and due to expansion of the effective tube diameter and hence loss of stress due to decrease in Φ_{ST} (the second term on the right side of eq 29).

Equation 30 can be converted to expressions for the storage and loss moduli G' and G'' using standard formulas:

$$G'(\omega)/G_N^0 = \int_0^1\frac{\omega^2 t'^2}{1+\omega^2 t'^2}\Phi_{ST}(t')\,\mathrm{d}\Phi(t') + \int_0^1\frac{\omega^2 t'^2}{1+\omega^2 t'^2}\Phi(t')\,\mathrm{d}\Phi_{ST}(t') \tag{31}$$

$$G''(\omega)/G_N^0 = \int_0^1\frac{\omega t'}{1+\omega^2 t'^2}\Phi_{ST}(t')\,\mathrm{d}\Phi(t') + \int_0^1\frac{\omega t'}{1+\omega^2 t'^2}\Phi(t')\,\mathrm{d}\Phi_{ST}(t') \tag{32}$$

Equations 31 and 32 generalize expressions by Milner et al.[29]

This completes the specification of the algorithm. Since it is an explicit time-integration method, the computer code is very robust and fast; run times of less than a second are typical for simple one- or two-component melts. In addition, the run time increases only linearly with the number of molecular species; runs involving as many as a thousand different molecular

species still typically require no more than a minute on a workstation.

IV. Parameters and Predictions

With a general algorithm in hand, the next step must be to test it against experimental data. To do this, we select 1,4-polybutadiene as a model compound, because there is a substantial body of literature data on well-characterized polybutadiene melts of various architectures and compositions: (1) "monodisperse" linears, (2) "bidispersed" linears, (3) "monodisperse" stars, (4) mixtures of "monodisperse" linears and stars, (5) "monodisperse" pom-poms, and (6) "monodisperse" combs. We use quotes in reference to "monodispersity" and "bidispersity", because, while the polymers were anionically synthesized, and are therefore theoretically rather sharp fractions, there is inevitably some dispersity to the distributions. We note that only the pom-poms and combs have backbone segments, whose relaxation involves branch-point motion. Thus, only for these architectures does the naive model for branch-point motion described in section III.D come into play.

A. Parameter Values. Besides the plateau modulus, which is tabulated for various polymers in Fetters et al.,[30] the theory presented here has as parameters two time constants τ_e and τ_0, which appear in eqs 6 and 26′. The equilibration time τ_e can be computed from the monomeric friction coefficient ζ_0, and for polybutadiene a value of ζ_0 at 25 °C can be obtained from Ferry.[31] From this, Pattamaprom et al.[32] obtain $\tau_e = 1.51 \times 10^{-6}$ s at 25 °C. The polybutadiene data from the literature to which we shall refer was taken at temperatures ranging from 24.5 to 30 °C; using time−temperature shifting and Ferry's WLF parameters,[30] we can account for this modest variation in temperature by allowing τ_e to vary from 1.51×10^{-6} s for both 24.5 and 25 °C to 1.37×10^{-6} s at 27 °C to 1.31×10^{-6} s at 28 °C to 0.931×10^{-6} s at 30 °C.[31]

With τ_e thus determined a priori, only τ_0 is left as a "free" parameter of our theory. In principle, τ_0 can be related to τ_e, since arm fluctuations are governed by the same monomeric friction that controls reptation. Pattamaprom et al. showed that a theoretically computed prefactor for arm fluctuations can give good a priori predictions of star arm relaxation. However, the nearly quantitative predictions achieved by Pattamaprom et al. required consideration of corrections to the arm-fluctuation prefactor due to fast "early-time" shallow-fluctuation Rouse modes, analyzed first by Milner and McLeish.[22] In particular, both Milner and McLeish[22] and Pattamaprom et al.[32] constructed crossover functions by which the prefactor for arm fluctuations was converted from the fast nonactivated form to an activated form at a particular point during the arm relaxation. In the case of the calculations of Pattamaprom et al., use of this crossover function, combined with theoretical values for the parameters, allowed predictions to be made for star polybutadienes without invoking any adjustable parameters at all. While a crossover prefactor could probably be constructed for use in the theory proposed here, we will forego this encumbrance, since our aim at this juncture is not precisely accurate predictions of star relaxation, but rather semiquantitative prediction by a *single algorithm* of the viscoelasticity of melts composed of arbitrary mixtures of branched species. Only if our algorithm is successful in this will it warrant the fine-tuning necessary to take account of more subtle issues.

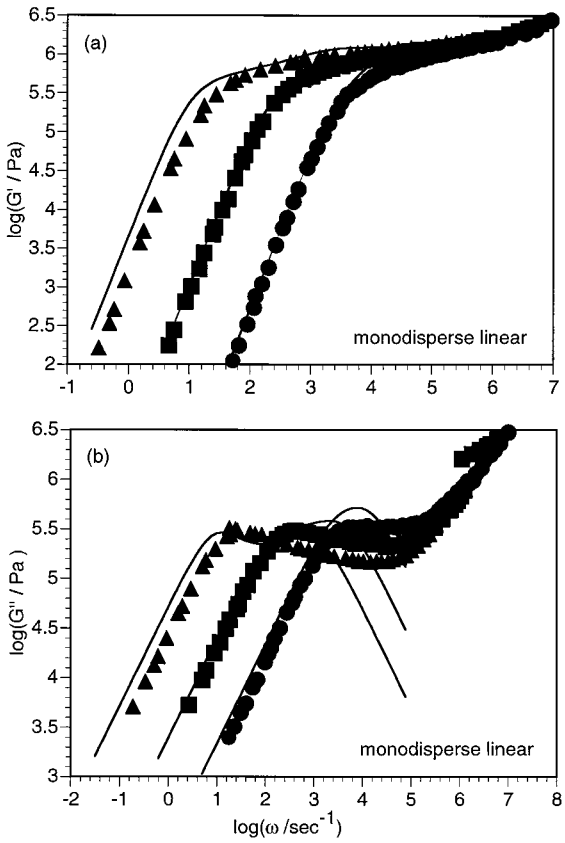

Figure 6. Comparison of predictions and measurements of (a) G' and (b) G'' for monodisperse linear polybutadienes of molecular weights, from right to left, of 20 700, 44 100, and 97 000 at 28 °C. In this and following figures, the symbols are experimental data and the lines are model predictions. The data are from Baumgaertel et al.[33]

Hence, it best suits our present purposes to avoid an overly detailed a priori calculation of the arm prefactor, so we instead use τ_0 as a fitting parameter, whose value is obtained from fits to data for monodisperse star polymers. In this way, we obtain the value $\tau_0 = 7 \times 10^{-6}$ s at 27 °C, a value that we adjust slightly with temperature using the same time−temperature shifting factors as were used to adjust τ_e.

With this specification, we will consider the model parameters fixed for purposes of this paper and content ourselves to compare its predictions with available data for well-characterized polymers, without further tinkering. In this regard, we remind the reader that the model is in many ways unrefined; we have already noted that the formulas for the waiting time, eq 16, and for the reptation time, eq 26′, are probably in need of improvement if quantitative predictions are to be obtained. Such refinements may prove worthwhile, if the model predictions given in what follows are deemed sufficiently promising.

B. Predictions. Figures 6−13 compare the predictions of the model with experimental data for (1) monodisperse linear polymers, (2) monodisperse star polymers, (3) bidisperse linear polymers, (4) blends of monodisperse linear and star molecules, (5) six-arm pom-poms, and (6) a 22-arm comb.

As remarked earlier, the only adjustable parameter in this comparison is τ_0, the coefficient of the star relaxation time, which was fit using the monodisperse star data[34] in Figure 7. Overall, the agreement between theory and experiment in Figures 6−13 is very promis-

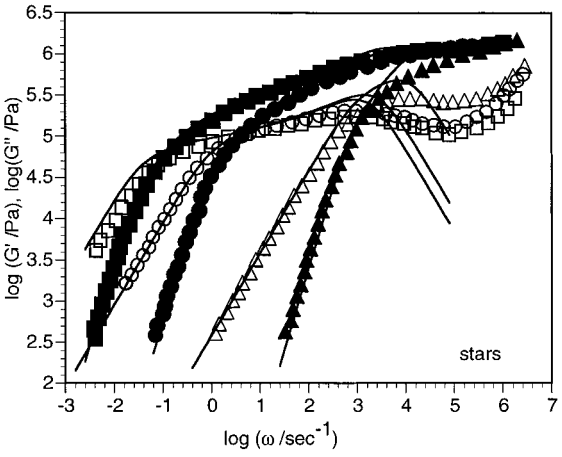

Figure 7. Comparison of predictions and measurements of G' (filled symbols) and G'' (unfilled symbols) for monodisperse polybutadiene 4-arm stars of molecular weights, from right to left, of 45 200, 121 000, and 162 000 at 27 °C. The data are for samples F, D, and B of Roovers.[34]

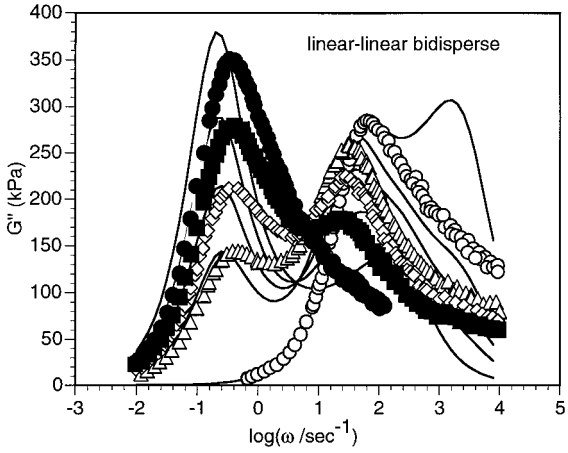

Figure 8. Comparison of predictions and measurements of G'' for bidisperse polybutadiene linear melts containing molecular weights 70 900 and 335 000 mixed at long-chain volume fractions of 0.0, 0.638, 0.768, 0.882, and 1.0 at 30 °C. The data are from Rubinstein and Colby.[35]

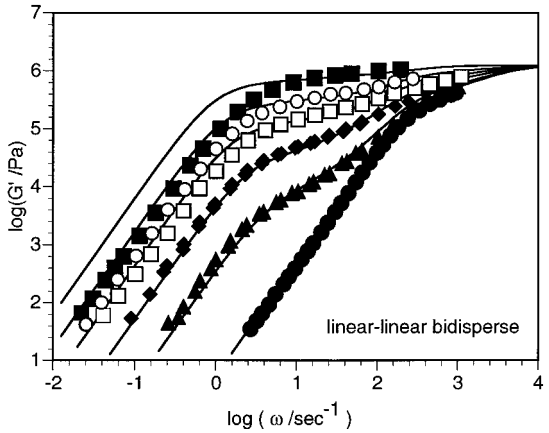

Figure 9. Comparison of predictions and measurements of G' for bidisperse polybutadiene linear melts containing molecular weights 39 000 and 181 000 mixed at long-chain volume fractions of 0.0, 0.1, 0.3, 0.5, 0.7, and 1.0 at 25 °C. The data are from Struglinski et al.[36]

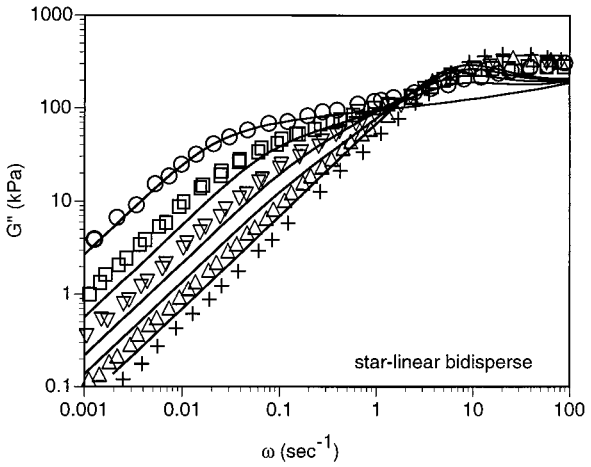

Figure 10. Comparison of predictions and measurements of G'' for bidisperse polybutadiene star-linear blends containing linear molecules of molecular weight 100 000 and three-arm stars of molecular weight 127 000 at star volume fractions (from right to left) of 0.0, 0.2, 0.5, 0.75, and 1.0 at 25 °C. The data are from Struglinski et al.[37]

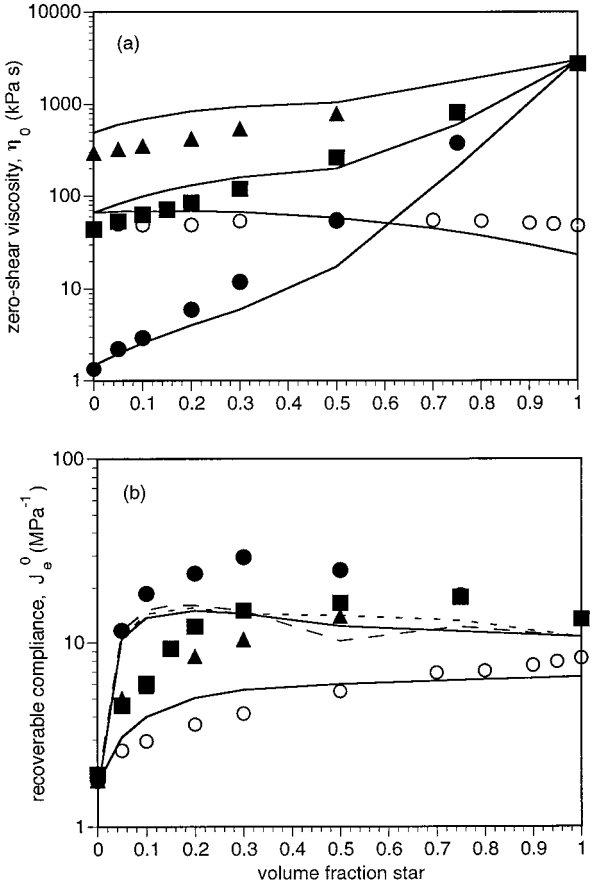

Figure 11. Comparison of predictions and measurements of (a) zero-shear viscosity η_0 and (b) recoverable compliance J_e^0 for bidisperse polybutadiene star-linear blends as functions of volume fraction star. The solid symbols are for mixtures of a three-arm star of molecular weight 127 000 with linear polymers of molecular weights 36 800, 100 000, and 168 000. The open symbols are for mixtures of a three-arm star of molecular weight 74 600 with a linear polymer of molecular weight 100 000. All data are at 25 °C from Struglinski et al.[37]

ing. For the monodisperse linear polymers[33] in Figure 6, the predictions of $G'(\omega)$ are excellent, except for a small deviation for the highest-molecular-weight polymer. For G'', the agreement is also excellent, except that the predicted high-frequency behavior deviates substantially from the measurements, which is expected because the model neglects both the "early-time" fast fluctuation mode and the high-frequency Rouse contri-

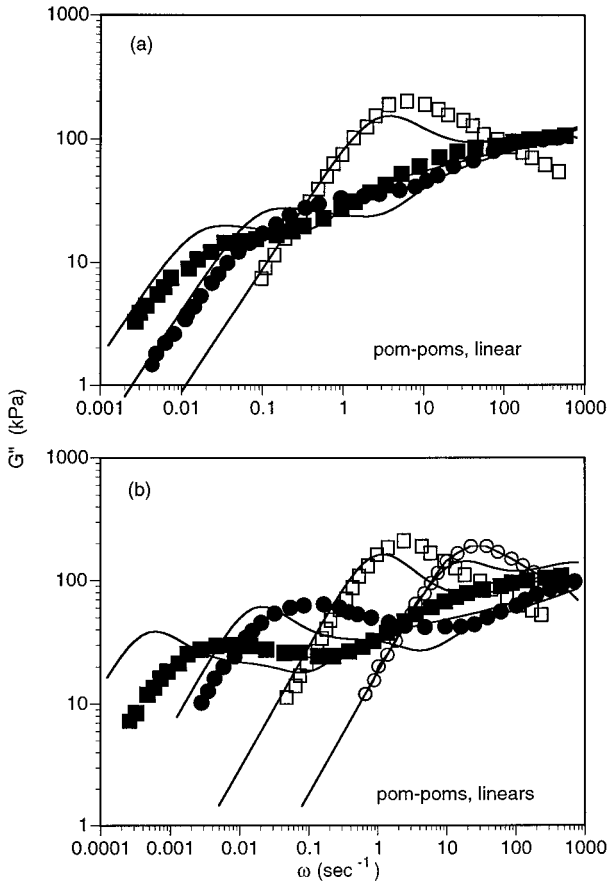

Figure 12. Comparison of predictions and measurements of $G''(\omega)$ for six-arm polybutadiene pom-poms (filled symbols) and linears (unfilled symbols) at 24.5 °C. In (a), the linear sample has a molecular weight of 129 000, while the pom-poms are P1134 (filled circles) and P1132 (filled squares). In (b), the linear samples have molecular weights, from right to left, of 86 500 and 176 000, while the pom-poms are P1210 (filled circles) and P1207 (filled squares). The molecular structures of the pom-poms are given in Table 2. The predicted moduli were reduced by a factor of 2 to match the observed plateau modulus in $G'(\omega)$ (not shown). The data are from Archer and Varshney.[38]

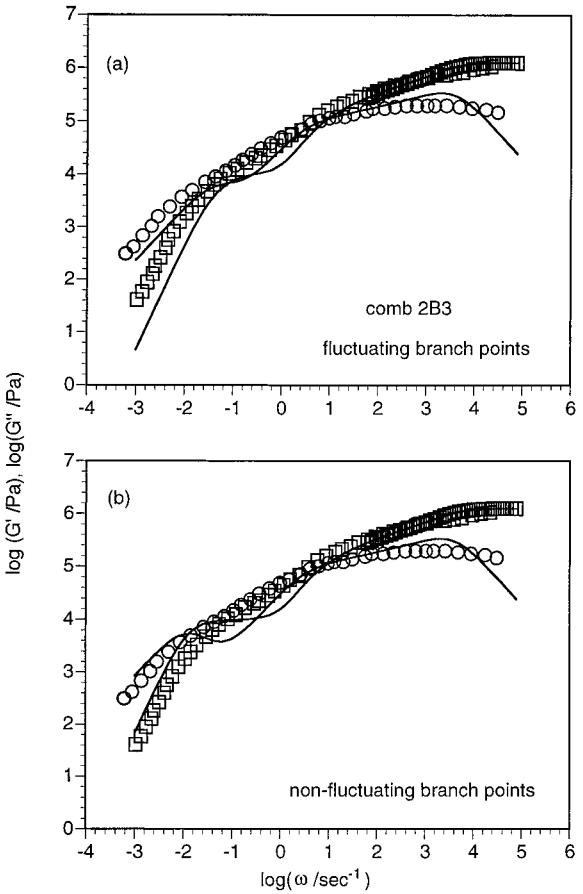

Figure 13. (a) Comparison of predictions and measurements of $G'(\omega)$ and $G''(\omega)$ for a 22-arm polybutadiene comb LC2B3 (see Table 2) studied by Roovers and Toporowski[39] at 27 °C. In (b), the theory lines were obtained by shutting off branch-point fluctuation.

butions, both of which contribute significantly to $G''(\omega)$ at high frequencies ω.[23,32] Neglect of these contributions to $G''(\omega)$ also leads to deviations between experiment and theory in Figures 7−9.

Apart from this, the agreement between theory and experiment for monodisperse stars in Figure 7 is essentially perfect.

The results for $G''(\omega)$ for linear−linear bidisperse blends[35] are plotted on a log−linear scale in Figure 8. Agreement is again good, except at high frequency. Note that, for the pure short linear polymer, G'' is predicted to have a double maximum, which as absent from the data. The higher-frequency maximum of these two is produced by the sudden onset of fluctuations at a time (or inverse frequency) equal to the short-chain prefactor $\tau_0 S_a^{3/2}$. This spurious high-frequency maximum is not present when "early-time" fluctuations are considered.[32] Additional data on binary blends of linear polybutadienes are available in Struglinski et al.[36] A comparison of the theory with these data for $G'(\omega)$ in Figure 9 again shows good agreement, but, as before, the theory overpredicts the low-frequency G' at high molecular weights.

Data from Struglinski et al.[37] and predictions of $G''(\omega)$ are shown in Figure 10 for star-linear blends with star volume fractions of 0, 0.2, 0.5, 0.75, and 1.0. Except at high frequencies, the agreement is again essentially perfect for the pure star polymer and is reasonable, though not perfect, for the mixtures.

Struglinski et al.[36] have tabulated values for the zero-shear viscosity η_0 and the recoverable compliance $J_e^0 \equiv (1/\eta_0^2) \lim_{\omega\to 0}[G'(\omega)/\omega^2]$ for four sets of star-linear 1,4-polybutadiene blends, namely, blends of linear chains of molecular weights 36 800, 100 000, and 168 000 with three-arm stars of molecular weights 74 600 and 127 000. Using these molecular weights, we obtain from our general algorithm plots of η_0 and J_e^0 vs star volume fraction ϕ_b and compare them to the experimental data in Figure 11. Note in Figure 11a that the zero-shear viscosities are reasonably well predicted over a wide range of conditions. In particular, for the two cases in which the pure linear chain is much less viscous than the pure star with which it is blended, the theory correctly predicts that the slope of the plot of log η_0 vs volume fraction increases with increasing ϕ_b; i.e., the lines are concave upward, as observed experimentally.

The recoverable compliance in Figure 11a is less well predicted by the theory. The algorithm does correctly predict that J_e^0 rises rapidly as ϕ_b increases from zero to around 0.1, but according to the algorithm, $J_e^0(\phi_b)$ for the mixtures is nearly independent of the molecular weight of the linear chain in the mixture, while in the experiments, the lower the molecular weight of the linear chain, the higher the value of J_e^0 for mixtures of that chain with a given star molecule, for $\phi_b < 0.5$.

Table 2. Polybutadiene Pom-Poms and Combs

polymer sample	polymer type	$M_w \times 10^3$	$M_b \times 10^3$	$M_a \times 10^3$	n_a	η_0 (Pa s) (exp)	η_0 (Pa s) (theory) (with fluct)	η_0 (Pa s) (theory) (without fluct)
P1134	pom-pom	135.8	47	14.8	6			
P1132	pom-pom	164	47	19.5	6			
P1210	pom-pom	162.7	90.7	12	6			
P1207	pom-pom	207.7	90.7	19.5	6			
LC3B4	comb	177	50	7.1	17.9	2.1×10^4	6.7×10^3	3.6×10^4
LC1B3	comb	256	50	11.3	18.1	6.5×10^4	2.1×10^4	1.0×10^5
LC2B4	comb	464	50	23.2	17.8	5.4×10^5	3.7×10^5	1.5×10^6
LC2T3	comb	336	50	23.2	12.3	4.0×10^5	1.2×10^6	5.0×10^6
LC2B3	comb	553	50	23.2	21.7	5.6×10^5	2.3×10^5	8.4×10^5

The data and predictions of $G''(\omega)$ for pom-poms having three arms at each end of a linear backbone are shown in Figure 12a,b (filled symbols), along with predictions and data for three linear polymers (unfilled symbols) studied by the same workers, Archer and Varshney.[38] The molecular weights of arms and backbones of these pom-poms are given in Table 2. Both these linear molecules and the backbones of the pom-poms were not predominantly 1,4-polybutadiene but contained around 50% 1,2-addition. This presumably explains the lower plateau moduli observed for these polymers compared to that for 1,4-polybutadienes. Here, we have corrected for this effect by merely shifting the predicted G' and G'' values downward by a factor of 2, with no other changes. This yielded good agreement between the predicted and measured $G'(\omega)$ values in the plateau region (not shown). After this adjustment in plateau modulus, the agreement of the theory with the experimental data for the linear polybutadienes (unfilled symbols) is good. For the pom-poms, the agreement is also good, except for the case of the largest pom-pom, whose terminal time is predicted to be about a factor of 5 too large. There is also more "rounding" in the experimental data and not as abrupt a transition into the terminal regime as predicted. We suspect that polydispersity, either in pom-pom arm lengths or in the number of arms per molecule, may account for this latter deviation between theory and experiment.

The predictions for G' and G'' are compared to data for a 22-arm polybutadiene comb, LC2B3, studied by Roovers and Toporowski,[39] in Figure 13a. The shape of the predicted G' and G'' curves are in reasonable agreement with the experiments, but the longest relaxation time and zero-shear viscosity are about a factor of 3 smaller than the measured values. Figure 13b presents predictions from the model derived by turning off branch-point fluctuations. That is, in Figure 13b, the branch points are only permitted to move in the reptation step described in section III.E. This increases the relaxation time and zero-shear viscosity by a factor of about 4 and produces better agreement with the experimental data. Table 2 compares the measurements of the zero-shear viscosities of other combs studied by Roovers and Toporowski with predictions of the model both with and without branch-point fluctuations. Notice that, for each sample except LC2T3, the experimental viscosity lies between the values predicted with and without branch-point fluctuation.

Overall, we believe that the predictions of the model are reasonably good, especially considering the range of structures covered, that there is only one adjustable parameter, and this was fixed using data for pure stars. We believe that the model is sufficiently accurate that we can now use it to predict trends in the dependencies of rheological properties on the branch content and branch type.

V. Effect of Polydispersity on Comb Rheology

Since our algorithm is general, we can consider structures that are not ideal, i.e., that are polydisperse in arm and backbone lengths. To do this, we reconsider the comb molecule LC2B3 studied in Figure 13a, which is defined by $M_b = 50\,000$, $M_a = 23\,200$, and $n_a = 22$. In Figure 13a, the theory assumed that the arms and backbones are perfectly monodisperse in molecular weight, that each molecule contains an equal number of arms, and that the arms are evenly spaced along the backbone; i.e., that the melt contains only one perfect molecular structure. Of course, no synthesis can attain such perfection, and in reality, we expect the arms and backbone to be at least slightly polydisperse, the arms to be unevenly distributed along the backbone, and the number of arms to vary from molecule to molecule. Since our algorithm was designed precisely for such situations, we now explore its predictions of the effects of such nonidealities. We allow the arms to be polydisperse with a log-normal distribution with M_{wa}/M_{na} values ranging from 1.001 to 2, and we set the weight-average arm molecular weight M_{wa} as 23 200 and weight-average number of branches n_{wa} as 22. We also allow the backbone to be log-normally polydisperse with M_{wb}/M_{nb} of 1.001 to 2.0 and $M_{wb} = 50\,000$. We assume that each arm chosen randomly from its distribution can attach to a backbone position with equal probability per unit length of backbone. This means that the number of arms per backbone for a monodisperse backbone will vary according to a Poisson's distribution, while for a polydisperse backbone, the longer backbones will typically contain more arms than the shorter ones. We generate a distribution of 2000 different molecular structures using these statistics and compute the linear rheology of the mixture.

Figure 14 shows the effect of polydispersity in arm and backbone molecular weights on the $G''(\omega)$ curves. For these calculations, we have turned off the branch-point fluctuations. Note that when polydispersity is added to the backbone while keeping the arm polydispersity low, the terminal time is reduced, while the high-frequency behavior is unchanged from that of the nearly monodisperse melt; see the bold dashed curve. Notice also that the "dimple" in G' at $\log(\omega)$ around unity in the predictions of Figure 14 is reduced or eliminated by addition of backbone polydispersity. When, however, polydispersity is added to the arms, while keeping the backbone almost monodisperse, the high-frequency modulus is reduced, and *a low-frequency tail appears that has a much longer terminal time than when the polydispersity is added to the backbone;* see the thin solid line. This low-frequency tail is produced by the "hierarchical effect"—long arms are very slow to relax and this propagates to the molecules containing those long arms, thus increasing the longest relaxation

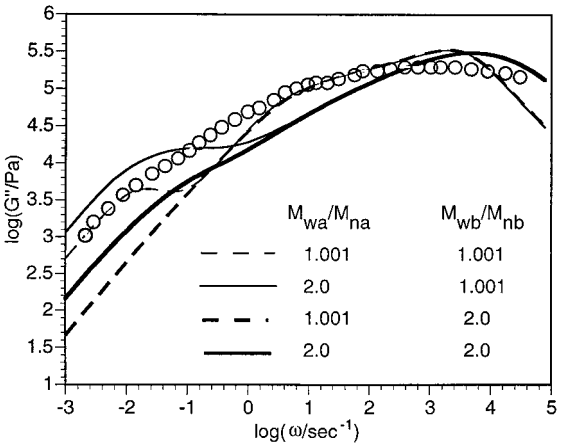

Figure 14. Predictions of $G''(\omega)$ for hypothetical comb LC2B3 with indicated polydispersities in the arm and backbone molecular weights, with random placement of arms along the backbones. For reference, the data for LCB3 are also included.

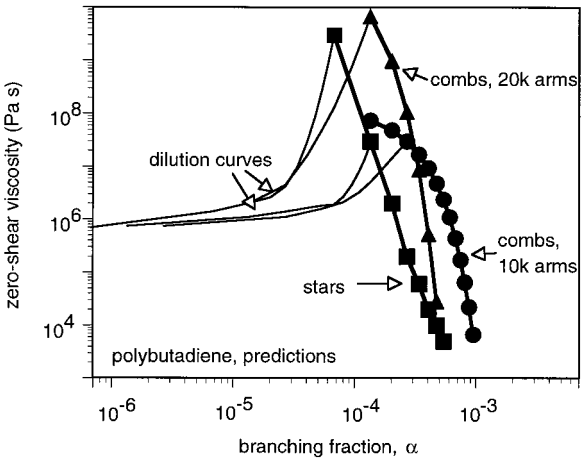

Figure 15. Predicted zero-shear viscosities for branched polybutadiene with weight-average molecular weight of 200 000 as a function of the fraction of carbons that are branch points. The squares are predictions of pure monodisperse star polymers of functionalities from 3 to 10, with each branch after the second counting as one "branch point". The circles are for monodisperse combs with arm molecular weight 10 000 and 3−16 arms; the triangles are for combs with arm molecular weight 20 000 with 3−8 arms. The thin lines are for blends of stars and combs with linear polymer of molecular weight 200 000. In this, and all subsequent figures, the temperature is taken to be 25 °C.

time. When polydispersity is added to both the arms and backbone, the curve has a shape that matches the shape of the experimental curve, except at very high frequency. While at this stage the model is not accurate enough to attempt to infer arm and backbone polydispersities from fits to the data, this exercise does illustrate the possibility that this might become possible, once a more refined model is available.

Areas where improvements are probably needed to make the model truly quantitative include (1) the formula for the reptation time eq 26′, (2) the expression eq 16 for the pause due to collapsed arms, (3) the magnitude of the primitive-path fluctuations governed by eq 4, (4) the degree of dynamic dilution allowed by the model, and (5) the omission of early-time primitive-path fluctuations.

VI. Effect of Branching Type on Zero-Shear Viscosities

Using the theory developed in section III and partially validated in section IV, we now predict zero-shear viscosities as a function of branching degree for various types of branched polybutadiene melts that are *monodisperse* in overall molecular weight. Figure 15 compares predictions of the zero-shear viscosity η_0 for monodisperse stars, combs, and mixtures of monodisperse stars and combs with linear polybutadienes of the same molecular weight, namely 200 000. These predictions are obtained from the algorithm presented in section III.

In Figure 15, the thick lines connecting symbols represent pure single-component branched polymers, either stars or combs. For the case of pure stars (squares), the branching fraction is controlled by varying n_a, the number of branches per molecule, ranging from $n_a = 3$ to 10. We count each branch beyond the second as contributing an effective "branch point" so that the number of branch points per molecule is $n_a - 2$; that is, we pretend that the branches actually emanate from closely spaced, but different, carbon atoms. Hence, α increases with increasing functionality. Note in Figure 15 that the viscosity decreases rapidly with increasing functionality and hence with increasing α. This occurs because for fixed total molecular weight, the branch length decreases with increasing n_a, and the viscosity of a star polymer in theory (and, for the most part, also in reality) depends only on the molecular weight of the arms and not on the number of arms.[40] Thus, the molecular weight of each arm decreases from 200 000/3 = 67 000 to 200 000/10 = 20 000, and this produces a large reduction in viscosity, since the viscosity of a star melt is exponential in the arm molecular weight.

The filled circles in Figure 15 are for comb molecules of total molecular weight 200 000 and with arms of molecular weight 10 000, with the number of arms n_a varying from 3 to 16. The increasing number of arms, each of fixed molecular weight, under conditions of fixed total molecular weight, implies that the backbone molecular weight decreases with increasing n_a. This decrease in backbone molecular weight produces a decrease in viscosity η_0 with increasing n_a, and therefore also with increasing α, as shown. However, for each value of α, such a comb has a viscosity higher than that of a star. The filled triangles in Figure 15 are again for comb molecules of total molecular weight 200 000, this time with arms of molecular weight 20 000, and number of arms n_a varying from 3 to 8. A decrease in η_0 with increasing α is again obtained, but the dependence of viscosity on α is much steeper than for the comb with shorter arms, and there is a crossover in the curves of η_0 vs α for the two different combs.

The thin lines without symbols in Figure 15 are predictions for blends of two stars and of two different comb molecules with linear polybutadiene, also of molecular weight 200 000. Thus, for example, by adding a linear polymer of molecular weight 200 000 to the three-arm star, the value of α is reduced in proportion to the weight fraction ϕ_L of added linear molecule. The viscosity decreases as linear molecules are added, eventually attaining that of pure linear polymer when $\phi_a = 1 - \phi_L$ approaches zero and therefore when α approaches zero. Analogous behavior is found for 6-arm comb molecules of arm molecular weight 10 000 and for 4-arm combs (really "H" molecules) of arm molecular weight 20 000.

As a whole, the qualitative pattern of the dependence of η_0 on α depicted in Figure 15 matches that predicted

by the Janzen−Colby formula, depicted in Figure 2. For both examples, that of randomly branched polyethylene of weight-average molecular weight 200 000 and of regularly branched polybutadiene of molecular weight 200 000, there is a maximum in zero shear viscosity at a branching fraction, α, of about 7×10^{-5}, and a steep decrease in viscosity for α in excess of this. Since polyethylene has a molecular mass of 14 per backbone carbon and polybutadiene has a molecular mass of 13.5 per backbone carbon, the value $\alpha = 7 \times 10^{-5}$ corresponds, for both polyethylene and polybutadiene, to a single branch point per molecule. Thus, as one converts unbranched molecules to branched molecules at fixed molecular weight, the viscosity of the melt rises until there is on average roughly one branch per molecule. Continued addition of branches leads to a decline in viscosity. Qualitatively, addition of the first branch to a linear chain quenches reptation and enormously slows the molecule's relaxation. Once one chain has been added, however, further addition of branches, at fixed molecular weight, in general decreases the molecular "span," or radius of gyration, reducing the molecule's degree of entanglement with its surroundings, thereby allowing it to relax faster.

This picture is only a gross one; Figure 15 shows that precisely defined branched polymers such as pure monodisperse stars, pure monodisperse combs, and mixtures of star and combs with linear melt can have very different viscosities, even for the same value of α and the same molecular weight. According to Figure 15, an enormous range of viscosity values η_0 are at least theoretically obtained even for melts which have identical molecular weight, identical branching fraction α, and are all perfectly monodisperse in molecular weight. For example, for a branching fraction of 2×10^{-4}, the viscosity can vary between 10^6 and 10^9 Pa s, depending on the particular branching architecture. Obviously, the few examples considered in Figure 15 could be multiplied many times over by varying the lengths and numbers of comb arms, by allowing star or comb arms to be heterogeneous in length, or by considering ternary mixtures of stars, combs, and linears. Thus, in reality, for a given value of α in the neighborhood of 10^{-4}, and a monodisperse molecular weight of 200 000, virtually any viscosity η_0 between 10^3 and 10^{10} Pa s could probably be obtained.

The results of Figure 15 suggest that branched polymers have zero-shear viscosities that are extraordinarily sensitive to the details of the branch distributions. This, in turn, implies that knowledge of the weight-averaged molecular weight and zero-shear viscosity of the product will be far from adequate for estimating the degree of branching, even if the product has been fractionated so perfectly that the fractions are monodisperse. This, in turn, suggests that Janzen and Colby's successful use of zero-shear viscosity to predict branching levels in randomly and rather lightly ($\alpha \leq 10^{-5}$) cross-linked linear polymers will not extend very well to more ideal or partially fractionated branched polymers. At least this is the case for the ideal monodisperse branched structures considered in Figure 2.

VII. Combinatorial Rheology

The difficulty we face in analyzing branched polymer rheology is one of *combinatorial complexity*. That is, there are many ways of arranging a given number of branches among molecules of a given molecular mass, and the viscosity of the resulting mixture of molecules is exquisitely sensitive to the branching arrangement. Deconvoluting branching information from the rheology is then an ill-posed problem in which there are too many parameters for the available data. Solution of this problem requires that additional data be obtained which can put additional constraints on the structures that are possible. Knowledge of the catalyst structure and catalytic mechanism is one source of additional constraints; a good kinetic model could, in principle, predict the mix of structures produced by a given catalyst. However, catalyst models have been slow in coming, and it is not likely that they will be general enough or accurate enough to completely and confidently define the structures without input or confirmation from analytic techniques applied to the product polymer. Analysis of sample fractions will certainly help overcome combinatorial complexity, but since traditional fractionation methods cannot separate molecules on the basis of their branching structure alone, they are not in themselves able to resolve the problem. Also, fractionation is expensive and time-consuming and usually results in small sample sizes, which limits the analytic tests that can subsequently be performed.

Given the limitations of other methods, it is natural to try to wring more information out of rheological data. There are a couple of fairly obvious ways this might be done. One way is to look at the entire linear viscoelastic frequency response and not just the zero-shear viscosity. Another source of additional rheological data is nonlinear viscoelasticity, such as extensional viscosity and shear step-strain data. Use of nonlinear data to characterize branching will require development of models for nonlinear viscoelasticity, which is an area of active research.[10,26,41]

Here, however, we suggest a third route for obtaining potentially large numbers of sets of additional rheological data that can be used to confront the problem of combinatorial complexity. We suggest performing rheological studies of partially characterized samples that have been strategically *blended* with fully characterized samples of known molecular weight and branching structure.

An illustration is given in Figure 16 for the simplest possible case of blending a linear polymer with each of two pure branched samples, both of molecular weight 200 000. One is a four-arm star, and the other a six-arm comb with an arm molecular of 10 000. These two branched samples have nearly the same zero-shear viscosity, around 3×10^7 Pa s. Each of these is blended with a linear polymer of molecular weight 200 000, and the predicted viscosity as a function of volume fraction comb or star is shown in Figure 16. Importantly, this figure shows that the star and comb polymers have very different *dilution curves*; on a semilog plot at volume fractions between 0.4 and 1.0 branched polymer, the curve for the star blend is concave up, and that of the comb blend is concave down. The concave-up shape predicted for star-linear blends for which the viscosity of the star is higher than that of the linear polymer is confirmed in the experimental data of Figure 11. Figure 17 shows that the concave-down pattern for comb/linear blends is predicted over a wide range of molecular weights of the linear polymers.

The most important aspect of these figures is that they illustrate how one might, at least in principle,

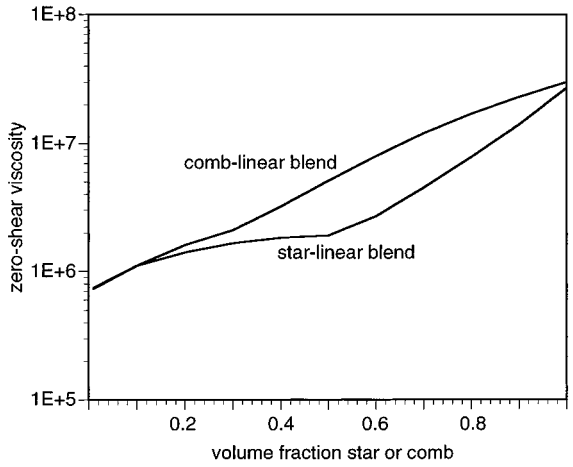

Figure 16. Predicted zero-shear viscosities of star/linear and comb/linear polybutadiene blends as a function of volume fraction star or comb. The star is a four-arm star, while the comb has six arms, each of molecular weight 10 000. Each species—star, comb, and linear—has a total molecular weight of 200 000.

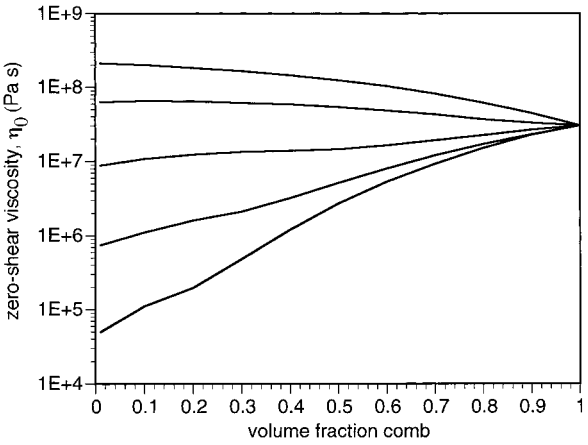

Figure 17. Predicted zero-shear viscosities of blends of a comb polybutadiene with six arms each of molecular weight 10 000 with linear polybutadienes of molecular weights 100 000, 200 000, 400 000, 700 000, and 1 000 000.

extract enough rheological data to confront the "combinatorial complexity" of incompletely characterized branching structures in commercial polymers. That is, by blending with a series of well-characterized linear polymers, star polymers, or other well-characterized model materials, one can multiply the number of rheological data to a degree limited only by experimental constraints, until, in theory, enough data are available to turn the ill-posed problem of branching structure into a well-posed problem. Of course, for each of potentially many blends, the entire linear viscoelastic curve can be measured and used to help determine the polymer structure.

Obviously, there are many impediments to implementing such a program. One such limitation is the imperfection of theories for branched polymer rheology. While the algorithm presented here is promising, it probably needs to be fine-tuned, or even thoroughly overhauled, to be made sufficiently quantitative for use as a characterization tool. Another impediment is the acquisition of data on large numbers of samples. There may well be ways of addressing this difficult problem as well. Most importantly, given unavoidable limitations on both experimental and theoretical accuracy, it is likely that different mixtures of branched species will give sufficiently similar rheological responses even in arbitrary blends with other polymers and that an unambiguous assignment of structure will be impossible unless constraints on the universe of possible structures are set, based on either catalyst chemistry or other information obtained a priori.

Thus, what we have presented here is by no means a complete solution to the "branched polymer problem". If anything, we have merely highlighted how truly difficult this problem really is. However, we can claim to have illustrated how, at least in principle, the large numbers of degrees of freedom present in the general "branched polymer problem" can be confronted by similarly large numbers of data points generated combinatorially from rheological data on mixtures of the unknown sample with well-characterized ones.

VIII. Summary and Prospective

A relatively simple algorithm is herein developed for predicting the linear viscoelasticity of arbitrary mixtures of various types of branched and linear molecules. The algorithm is shown to be semiquantitatively accurate in its predictions of experimental data for well-characterized polybutadiene linear, star, mixed linear and star, and, to some extent, for pom-pom and comb melts. The model shows that the zero-shear viscosity of a branched melt is extremely sensitive not only to degree of branching but also to type. The results suggest that information on the type of branching present in an imperfectly characterized polymer sample might be inferred by measuring the viscosity and other viscoelastic properties of blends of the branched sample with well-characterized linear, and possibly other well-characterized branched, samples. Since the blended component can be chosen arbitrarily, arbitrarily large numbers of data sets might thereby be obtained combinatorially and used to infer branching levels and types. Success of this method depends on the accuracy of the theory used to connect the molecular structures present in the melt to the linear viscoelastic data. Hence, to realize the potential of "combinatorial rheology", further development of accurate theories for the viscoelastic properties of complex branched polymer blends are required, as is the development of experimental methods that can extract rheological data rapidly from many samples.

Acknowledgment. The author is grateful for financial support from the National Science Foundation, Grant DMR9807262.

References and Notes

(1) Janzen, J.; Colby, R. H. *J. Mol. Struct.* **1999**, *485*−*486*, 569−583.
(2) Tuminello, W. H. *Polym. Eng. Sci.* **1986**, *26*, 1339−1347.
(3) des Cloizeaux, J. *Macromolecules* **1990**, *23*, 4678−4687.
(4) Tsenoglou, C. *Macromolecules* **1991**, *24*, 1762−1767.
(5) Wasserman, S. H.; Graessley, W. W. *J. Rheol.* **1992**, *36*, 543−572.
(6) Mead, D. W. *J. Rheol.* **1994**, *38*, 1797−1827.
(7) Shaw, M. T.; Tuminello, W. H. *Polym. Eng. Sci.* **1994**, *34*, 159−165.
(8) Milner, S. T. *J. Rheol.* **1996**, *40*, 303−315.
(9) McLeish, T. C. B. *Europhys. Lett.* **1988**, *B6*, 511−516.
(10) McLeish T. C. B.; Allgaier, J.; Bick, D. K.; Bishko, G.; Biswas, P.; Blackwell, R.; Blottiere, B.; Clarke, N.; Gibbs, B.; Groves, D. J.; Hakiki, A.; Heenan, R. K.; Johnson, J. M.; Kant, R.; Read, D. J.; Young, R. N. *Macromolecules* **1999**, *32*, 6734−6758.

(11) Padmanabhan, M.; Macosko, C. W. *Rheol. Acta* **1997**, *36*, 144−151.
(12) Laun, H. M. In *Proceedings of the Ninth International Congress on Rheology, Acapulco, Mexico, 1984*; p 419.
(13) Laun, H. M.; Schuch, H. *J. Rheol.* **1989**, *33*, 119−175.
(14) Wagner, M. H.; Bastian, H.; Hachmann, P.; Meissner, J.; Kurzbeck, S.; Münstedt, H.; Langouche, F. *Rheol. Acta*, submitted.
(15) Arnett, R. L.; Thomas, C. P. *J. Phys. Chem.* **1980**, *84*, 649.
(16) Raju, V. R.; Rachapudy, H.; Graessley, W. W. *J. Polym. Sci., Polym. Phys. Ed.* **1979**, *17*, 1223−1235.
(17) Gleissele, W. In *Rheology;* Astarita, G., Marrucci, G., Nicolais, L., Eds.; Plenum Press: New York, 1980; Vol. 2, pp 457−462.
(18) Mendelson, R. A.; Bowles, W. A.; Finger, F. L. *J. Polym. Sci., Polym. Phys. Ed.* **1970**, *8*, 105−126.
(19) Ram, A. *Polym. Eng. Sci.* **1977**, *17*, 793−798.
(20) Lusignan, C. P.; Mourey, T. H.; Wilson, J. C.; Colby, R. H. *Phys. Rev. E* **1999**, *60*, 5657−5669.
(21) Ball, R. C.; McLeish, T. C. B. *Macromolecules* **1989**, *22*, 1911−1913.
(22) Milner, S. T.; McLeish, T. C. B. *Macromolecules* **1997**, *30*, 2159−2166.
(23) Milner, S. T.; McLeish, T. C. B. *Phys. Rev. Lett.* **1998**, *81*, 725−728.
(24) Pearson, D. S.; Helfand, E. *Macromolecules* **1984**, *17*, 888−895.
(25) Doi, M.; Edwards, S. F. *The Theory of Polymer Dynamics;* Oxford University Press: New York, 1986.
(26) McLeish, T. C. B.; Larson, R. G. *J. Rheol.* **1998**, *42*, 81−110.
(27) Viovy, J. L.; Rubinstein, M.; Colby, R. H. *Macromolecules* **1991**, *24*, 3587−3596.
(28) Watanabe, H. *Prog. Polym. Sci.* **1999**, *24*, 1253−1403.
(29) Milner, S. T.; McLeish, T. C. B.; Young, R. N.; Hakiki, A.; Johnson, J. M. *Macromolecules* **1998**, *31*, 9345−9353.
(30) Fetters, L. J.; Lohse, D. J.; Richter, D.; Witten, T. A.; Zirkel, A. *Macromolecules* **1994**, *27*, 4639−4647.
(31) Ferry, J. D. *Viscoelastic Properties of Polymers*, 3rd ed.; Wiley: New York, 1980.
(32) Pattamaprom, C.; Larson, R. G.; Van Dyke, T. J. *Rheol. Acta*, in press.
(33) Baumgaertel, M.; De Rosa, M. E.; Machado, J.; Masse, M.; Winter, H. H. *Rheol. Acta* **1992**, *31*, 75−82.
(34) Roovers, J. *Polymer* **1985**, *26*, 1091−1095.
(35) Rubinstein, M.; Colby, R. H. *J. Chem. Phys.* **1988**, *89*, 5291−5306.
(36) Struglinski, M. J.; Graessley, W. W.; Fetters, L. J. *Macromolecules* **1985**, *18*, 2630−2643.
(37) Struglinski, M. J.; Graessley, W. W.; Fetters, L. J. *Macromolecules* **1988**, *21*, 783−789.
(38) Archer, L. A.; Varshney, S. K. *Macromolecules* **1998**, *31*, 6348−6355.
(39) Roovers, J.; Toporowski, P. M. *Macromolecules* **1987**, *20*, 2300−2306.
(40) Fetters, L. J.; Kiss, A. D.; Pearson, D. S.; Quack, G. F.; Vitus, F. J. *Macromolecules* **1993**, *26*, 647−654.
(41) Bick, D. K.; McLeish, T. C. B. *Phys. Rev. Lett.* **1996**, *76*, 2587−2590.

MA000700O